Granular Matter 5, 147–151 © Springer-Verlag 2003
DOI 10.1007/s10035-003-0143-9

Discrete element modelling of cyclic loading of crushable aggreates

O. Harireche, G.R. McDowell

Abstract This paper examines the discrete element modelling of cyclic loading of an aggregate of crushable sand grains. Each grain of sand is modelled as an agglomerate of balls bonded together. The aggregate is subjected to compaction followed by isotropic normal (plastic) compression, and then unloaded to half the maximum applied stress. The aggregate is then subjected to cyclic loading to a maximum stress ratio of 0.8. The aim of the paper is to examine the reduction of the rate of axial strain with number of cycles, and to determine the relative influences of volumetric strain and shear strain rates on the axial strain rate. In particular, the paper aims to show whether particle breakage is mainly related to the accumulation of volumetric strain. This is found to be the case, which is consistent with proposals by other authors that plastic hardening under monotonic loading is due to particle fracture.

Keywords Granular material, Grain crushing, Cyclic loading, Discrete element modelling

1 Introduction

It has been proposed [1–4] that for granular materials subjected to monotonic loading, particle fracture provides the mechanism for plastic hardening. Various parameters have been proposed to quantify the amount of breakage – see e.g. [5], and attempts have been made to relate this quantity to the isotropic preconsolidation pressure, which is assumed to be a function of plastic volumetric strain ("volumetric hardening" models). As yet, the authors know of no previous work which has examined the degradation of aggregates subjected to cyclic loading. This is because of the difficulty in measuring accurately the degradation caused by many cycles of load. The study of shakedown of granular materials has shown by Werkmeister et al. [6] that under low stress ratios and low stress levels, the rate of increase of axial strain in a triaxial sample subjected to conventional cyclic loading tends to zero (i.e. the material shakes down). Under high stress ratios, however, Werkmeister et al. [6] showed that plastic axial strain continued to accumulate and they proposed that grain abrasion or fracture may be responsible for such behaviour. However, they were unable to prove this hypothesis. This paper aims to model the cyclic loading of a crushable aggregate using the discrete element method, under stress conditions which do produce crushing, in order to ascertain the effect of crushing on the volumetric and shear strains within the sample. The discrete element method, developed by Cundall and Strack [7], uses spheres to model soil particles. In their original BALL model, balls could not be bonded together, but recent developments have made this possible via the program PFC3D [8]. Contact forces are used to calculate the accelerations of each ball using Newton's Second Law, and the accelerations are integrated to give velocities and displacements (and hence new contact forces via a contact constitutive law), via an explicit time-stepping scheme. It will be shown in this paper that particle breakage appears to be a strong function of volumetric strain but not of shear strain, and that the increase of axial strain with number of cycles in the sample is mainly due to volumetric strain and therefore bond breakage.

Received: 13 May 2003

O. Harireche, G.R. McDowell (✉)
School Civil Engineering, University of Nottingham,
University park, Nottingham NG7 2RD, UK
e-mail: Glenn.Mcdowell@nottingham.ac.uk

2 Discrete element modelling of crushable aggregates

McDowell and Harireche [9] showed that it was possible to model a sand particle as an agglomerate of many balls bonded together. They showed that it was also possible to reproduce the right average strength of agglomerates (measured by compression between flat platens) as a function of size, and the correct statistical distribution of strengths for a given size, so that the strengths followed the Weibull [10] distribution, and the numerical results were consistent with experimental data for Leighton Buzzard sand published by McDowell [11]. McDowell and Harireche [12] used their model agglomerates to study the one-dimensional normal compression of Leighton Buzzard sand by performing simulations of one-dimensional normal compression of aggregates of their agglomerates. They showed that it was possible to reproduce normal compression lines (on a plot of volume against logarithm of applied stress) of the correct form, and they were also able to demonstrate that their model correctly predicted the yield stress of the aggregate to be a function of particle (i.e. agglomerate) size. This work follows their work on monotonic one-dimensional loading, and aims to provide a study into the behaviour of crushable aggregates subjected to cyclic loading. For this purpose, the agglomerates used in [12] will be used in this paper. The aggre-

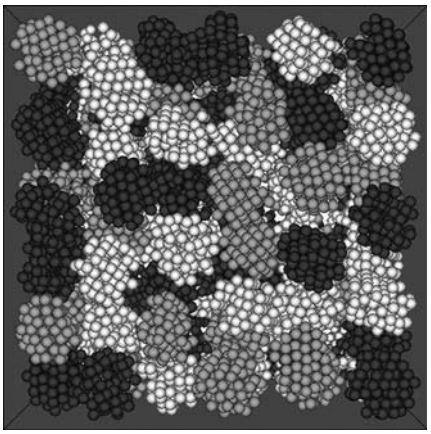

Fig. 1. Aggregate of 159 agglometrates of diameter 0.5 mm in a cubic triaxial cell of side 2.5 mm

gate (Figure 1) is composed of 159 approximately spherical agglomerates of diameter 0.5 mm. Each agglomerate is modelling a sand particle of size 0.5 mm. The sample dimensions of the true-triaxial specimen are 2.5 mm x 2.5 mm x 2.5 mm. Agglomerates are initially formed using 135 balls of diameter 0.074 mm bonded together by contact bonds in hexagonal close packing. Each agglomerate has then been subjected to a random rotation and flaws have been simulated by a random removal of 30 to 55% balls in the agglomerate. This also removes the regular geometric arrangement produced by hexagonal close packing. The range of the number of balls removed controls the statistical variation in agglomerate strength, and the range 30–55% was found by McDowell and Harireche [9] to give the desired Weibull modulus $m \approx 3$, which controls the variability in strength. The bond strength was selected in such a way to provide the correct average tensile strength.

3 Discrete element modelling of cyclic loading of crushable aggregates

The crushable aggregate described in the previous section (Figure 1) has six frictionless walls. Walls can be moved inwards or outwards to load or unload the sample, respectively. McDowell and Harireche [12] found that for their one-dimensional normal compression tests, the yield stress (measured as the point of maximum curvature on a plot of sample volume against logarithm of stress) was about 20 MPa. For the purposes of modelling cyclic triaxial loading, the sample was initially subjected to oedometric compaction by moving the top wall at a constant rate until a mean stress of 1MPa was reached, and then unloaded. The wall displacement rate was chosen to be sufficiently small so that quasi-static conditions were obtained. Figure 2 shows the evolution of mean and deviatoric stresses during this process and the irrecoverable volume reduction which is evident after unloading. No bond breakage was observed at this stage because of the low level of stress, relative to the yield stress of the aggregate. Following unloading, the sample was isotropically compressed using stress control. This involves using the servo-control procedure described in the PFC3D manuals [8], whereby wall

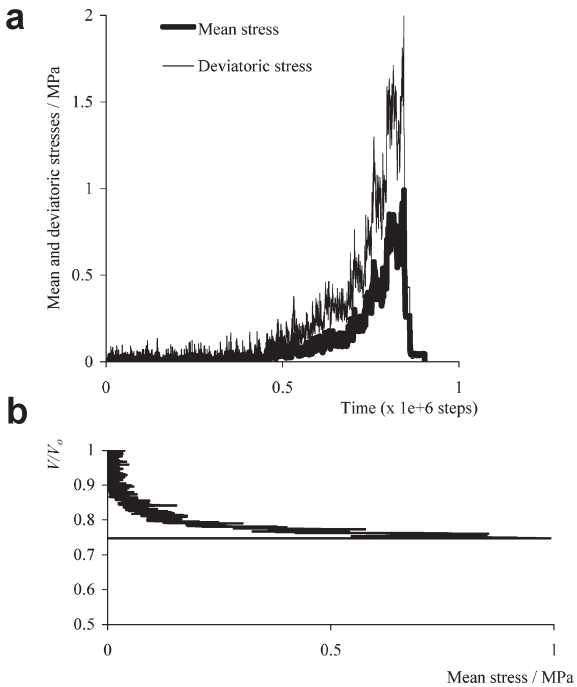

Fig. 2. (a) Mean and deviatoric stresses as functions of time during oedometic compaction and unloading. **(b)** Normalised volume as a function of mean stress during oedometric compaction and unloading

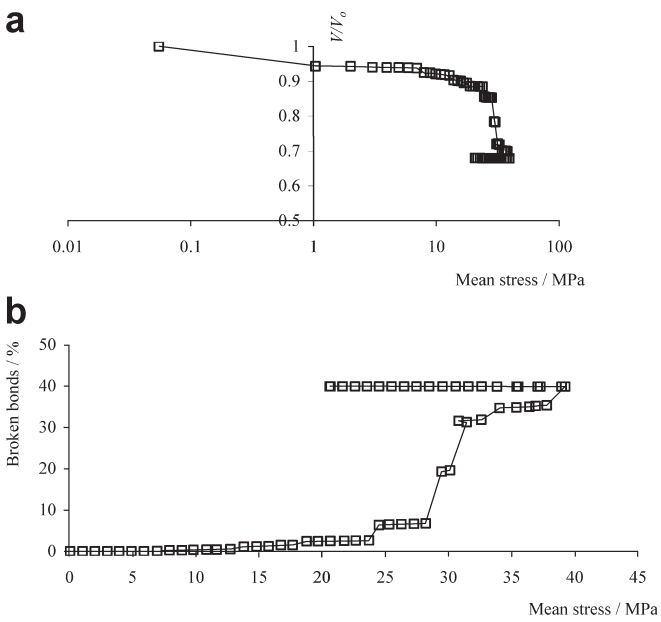

Fig. 3. (a) Normalised volume as a function of mean stress during isotropic normal compression and unloading. **(b)** Percentage of broken bonds as a function of mean stress during isotropic normal compression and unloading

velocities are adjusted to achieve a desired stress in such a way that they diminish as the target stress is reached. The servo-control mechanism was activated for the six walls in order to achieve an isotropic stress $p = 40$ MPa, which establishes an initial yield surface in deviatoric : mean effective stress space. The sample was then unloaded to a mean stress $p = 20$ MPa. Figure 3a shows the resulting compression curve in volume V : log stress σ

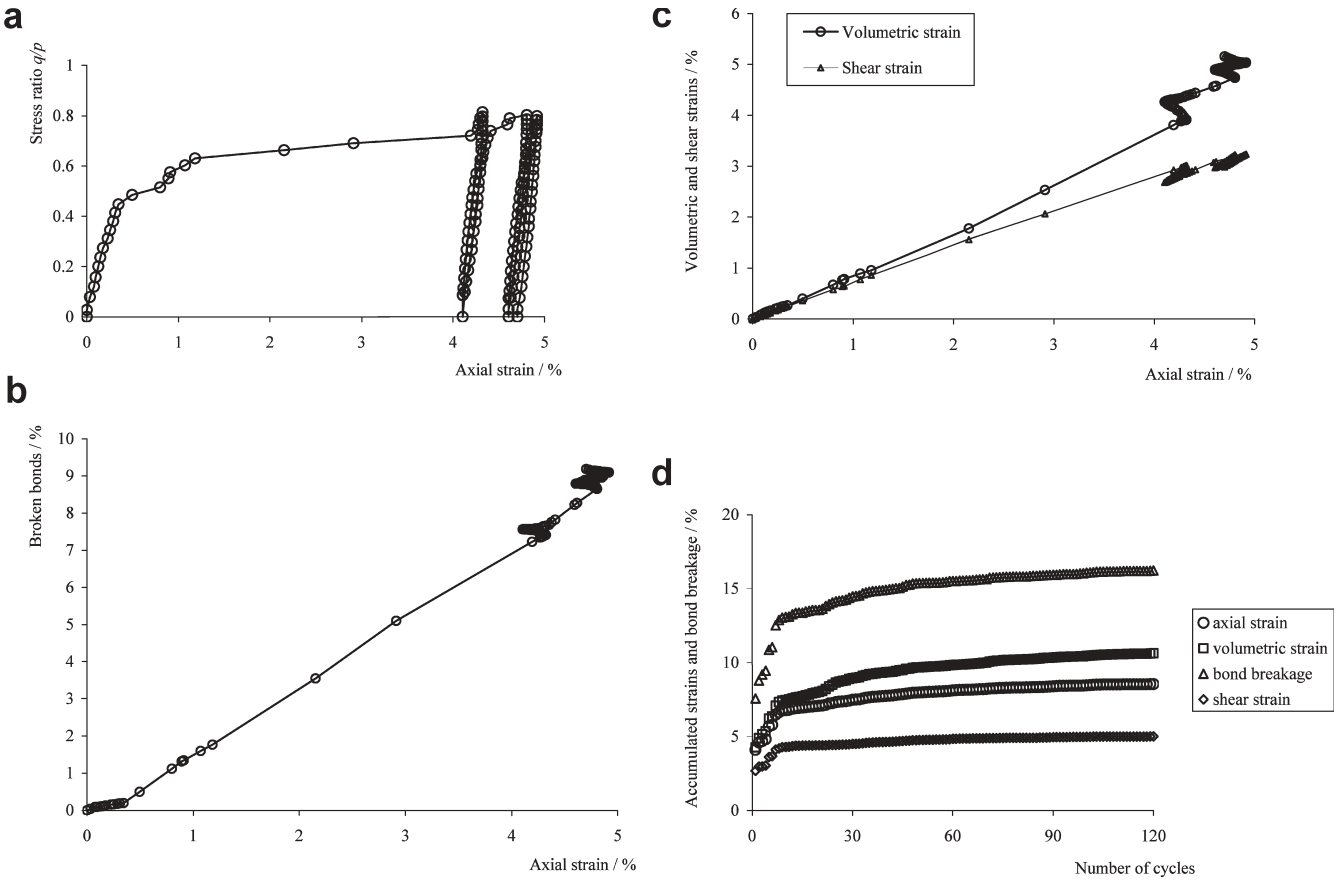

Fig. 4. (a) Stress ratio q/p versus axial strain during the 3 first cycles. **(b)** Percentage of broken bonds versus axial strain during the 3 first cycles. **(c)** Volumetric and shear strains versus axial strain during the 3 first cycles. **(d)** Accumulated strains and bond breakage versus number of cycles

space. The sample volume has been normalised by the initial sample volume V_o for clarity. Voids ratio is not used, because the agglomerates are porous, and when fracture occurs, internal voids become external voids. Figure 3b shows bond breakage plotted as a function of mean stress. The figure shows that the onset of bond breakage corresponds to an isotropic stress of approximately 13 MPa. Subsequent loading to 40 MPa caused approximately 40% bonds to break. It is worth noting that no bond breakage occurred during unloading. After unloading to 20 MPa, the sample was subjected to conventional (i.e. constant horizontal stress = 20 MPa) cyclic loading. During each cycle, the vertical stress was increased until a stress ratio of 0.8 was obtained. Stress ratio is defined as deviatoric stress $q = \sigma_1 - \sigma_3$ divided by mean stress $p = (\sigma_1 + 2\sigma_3)/3$. The sample was then unloaded back to isotropic conditions. The stress path was followed incrementally using the servo-control mechanism. For conventional triaxial tests $\Delta q = 3\Delta p$, and the increment in stress was chosen to be 1 MPa along the length of the stress path in $q : p$ space. The increment of vertical stress was achieved within a tolerance of 1% of the target value using servo-control of the top and bottom walls. The servo-control mechanism was also activated for the lateral walls to maintain a constant lateral confinement.

Figure 4a shows the stress ratio q/p, as a function of axial strain $\varepsilon_a$for the first 3 cycles. A small circle on the figure depicts the response reached after equilibrium of the granular assembly after each stress increment along the conventional triaxial stress path. Note that the axial strain occurring after completion of the first cycle is large compared to the axial strain that occurs during subsequent cycles. A small amount of bond breakage occurs during unloading for each cycle and this is accompanied by an increase in axial strain (Figure 4b). Figures 4c shows that on unloading, the bond breakage is accompanied by an increase in volumetric strain, but a reduction in shear strain (leading to the overall increase in axial strain in Figure 4b). This illustrates the important influence of bond breakage on volumetric strain. The contributions to axial strain ε_a from triaxial shear strain ε_q and volumetric strain ε_v are given by

$$\varepsilon_a = \varepsilon_q + \varepsilon_v/3 \tag{1}$$

where

$$\varepsilon_q = \frac{2}{3}(\varepsilon_1 - \varepsilon_3) \tag{2}$$

and

$$\varepsilon_v = \varepsilon_1 + 2\varepsilon_3 \tag{3}$$

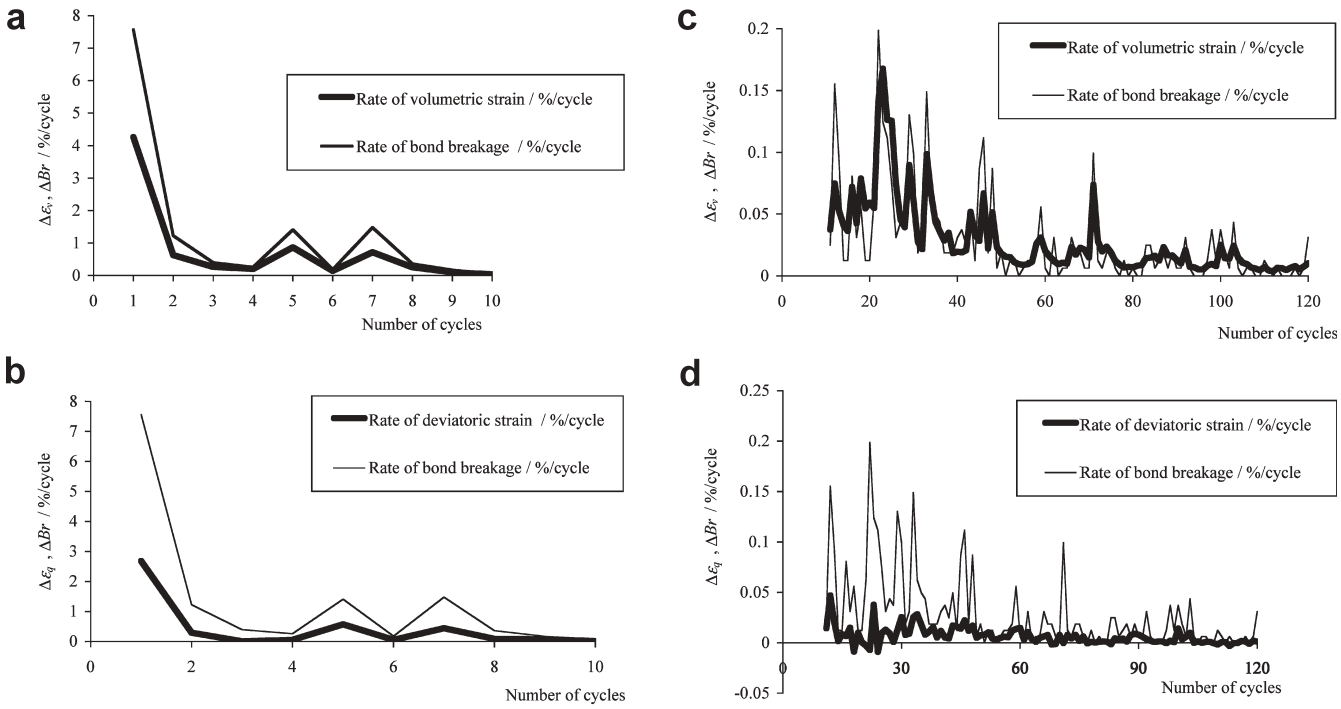

Fig. 5. Rates of volumetric strain $\Delta\varepsilon_v$, shear stain $\Delta\varepsilon_q$ and bond breakage ΔBr as functions of the number of cycles

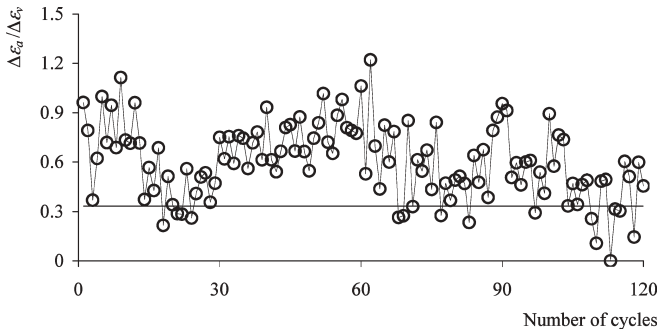

Fig. 6. Ratio of axial strain rate to volumetric strain rate as a function of the number of cycles

The relative contributions are evident in Figure 4d, which shows the accumulated strain at the end of each unload-reload cycle, together with the percentage of bonds broken, for a total of 120 cycles. Figure 4d shows that the strain rates and the rate of bond breakage appear to decrease as the number of cycles increases. This is investigated in Figure 5, which shows the rates of increase of volumetric strain $\Delta\varepsilon_v$ and shear strain $\Delta\varepsilon_q$ (i.e. increase in each strain per load-unload cycle) as a function of the number of cycles. The rate of bond breakage (increase in percentage of broken bonds per cycle) Δ Br is also shown for comparison. Because of the rapid decrease of the rates of strain and bond breakage to very small values after a few cycles, the rates are shown for the first 10 cycles in Figures 5a, b and for the remaining 110 cycles in Figures 5c, d. During the first 10 cycles, bond breakage is accompanied by both volumetric and shear strain. It is evident, however, in Figures 5c, d, that bond breakage correlates much better with volumetric strain than shear strain, and it seems that there is still a significant rate of bond breakage and volumetric strain even after 100 cycles, although the rate of shear strain is almost zero after about 70 cycles. This is confirmed in Figure 6, which shows the ratio of axial strain rate to volumetric strain rate as a function of the number of cycles. According to (1), this ratio should tend to 1/3 if shear strain rate tends to zero. This is evident in Figure 6, although there is some fluctuation in the values. It may thus be concluded that in this case, the ongoing accumulation of axial strain after a large number of cycles is due to volumetric strain, rather than shear strain, and is accompanied by bond breakage. It may thus be concluded that particle fracture is responsible for irrecoverable volumetric strain under cyclic loading.

4 Conclusions

The response of a crushable granular material to conventional triaxial cyclic loading has been investigated using the discrete element code PFC3D. The simulation models each sand particle as an agglomerate of bonded balls, and bond breakage has been found to play a key role in accumulation of axial strain. A study of the rates of volumetric and shear strains together with the rate of bond breakage shows that initially, significant volumetric and shear strains occur together with bond breakage. On first loading, the axial strain is mainly due to the large shear strain which occurs. However, as the number of cycles increases, the rate of shear strain tends to zero, so that the ongoing axial strain is due to volumetric strain, which is accompanied by bond breakage. It appears that bond

breakage provides the mechanism for irrecoverable volume reduction under cyclic loading.

References

1. G. R. McDowell & M. D. Bolton, Géotechnique, 48 (5) (1998), p. 667
2. I. K. Lee & M. R. Coop, Predictive soil mechanics, G. T. Houlsby & A. N. Schofield, (Eds.), Thomas Telford, London, (1993), p. 186
3. M. R. Coop & I. K. Lee, Géotechnique 45(1) (1995), p. 117
4. Y. Nakata, A. F. L. Hyde, M. Hyodo & H. Murata, Géotechnique 49(5) (1999), p. 567
5. B. O. Hardin, ASCE J. Geotech. Engng. 111(10) (1985), p. 1177
6. S. Werkmeister, A. R. Dawson, & F. Wellner, Transportation Res. Record 1757 (2001), p. 75
7. P. A. Cundall & O. D. L. Strack, Géotechnique 29(1) (1979), p. 47
8. Itasca, Particle Flow Code in Three Dimensions. Itasca Consulting Group, Inc., Minnesota, 1999
9. G. R. McDowell & O. Harireche, Géotechnique 52(2) (2002), p. 131
10. W. Weibull, J. Appl. Mech. 18 (1951), p. 293
11. G.R. McDowell, Soils and Foundations 42(1) (2002), p. 139
12. G. R. McDowell & O. Harireche, Géotechnique 52(4) (2002), p. 295